Carcinogenesis, 2015, Vol. 36, No. 11, 1372–1380

doi:10.1093/carcin/bgv110
Advance Access publication August 12, 2015
Original Manuscript

ORIGINAL MANUSCRIPT

Genetic ablation of caspase-7 promotes solar-simulated light-induced mouse skin carcinogenesis: the involvement of keratin-17

Mee-Hyun Lee[1,2,†], Do Young Lim[1,†], Myoung Ok Kim[1,3], Sung-Young Lee[1,5], Seung Ho Shin[1,6], Jae Young Kim[4], Sung-Hyun Kim[1,3], Dong Joon Kim[1,7], Sung Keun Jung[1,8], Ke Yao[1], Joydeb Kumar Kundu[9], Hye Suk Lee[2], Cheol-Jung Lee[2], Sally E.Dickinson[10], David Alberts[10], G.Timothy Bowden[10], Steven Stratton[10], Clara Curiel[10], Janine Einspahr[10], Ann M.Bode[1], Young-Joon Surh[5], Yong-Yeon Cho[1,2] and Zigang Dong[1,5,*]

[1]The Hormel Institute, University of Minnesota, 801 16th Ave. NE, Austin, MN 55912, USA, [2]College of Pharmacy, The Catholic University of Korea, 43, Jibong-ro, Wonmi-gu, Bucheon-si, Gyeonggi-do 420-743, South Korea, [3]Center for Laboratory Animal Resources, School of Animal BT Science and, [4]Department of Biochemistry, School of Dentistry, Kyungpook National University, Daegu 702-701, South Korea, [5]Department of Molecular Medicine and Biopharmaceutical Sciences, Graduate School of Convergence Science and Technology, College of Pharmacy, Seoul National University, Seoul 151-742, South Korea, [6]Program in Biomedical Informatics and Computational Biology, University of Minnesota, Minneapolis, MN 55455, USA, [7]Medical Genomics Research Center, Korea Research Institute of Bioscience and Biotechnology, Daejeon 305-806, South Korea, [8]Functionality Evaluation Research Group, Korea Food Research Institute, Seongnam 463-746, South Korea, [9]College of Pharmacy, Keimyung University, Daegu 704-701, South Korea and [10]University of Arizona Cancer Center, Tucson, AZ 85704, USA

*To whom correspondence should be addressed. Tel: +1-507-437-9600; Fax: +1-507-437-9606; Email: zgdong@hi.umn.edu

†These authors contributed equally to this work.

Correspondence may also be addressed to Yong-Yeon Cho. Tel: +82-2-2164-4092; Fax: +82-2-2164-4059; Email: yongyeon@catholic.ac.kr

Abstract

Solar ultraviolet irradiation is an environmental carcinogen that causes skin cancer. Caspase-7 is reportedly expressed at reduced levels in many cancers. The present study was designed to examine the role of caspase-7 in solar-simulated light (SSL)-induced skin cancer and to elucidate its underlying molecular mechanisms. Our study revealed that mice with genetic deficiency of *caspase-7* are highly susceptible to SSL-induced skin carcinogenesis. Epidermal hyperplasia, tumor volume and the average number of tumors were significantly increased in *caspase-7* knockout (KO) mice compared with SKH1 wild-type mice irradiated with SSL. The expression of cell proliferation markers, such as survivin and Ki-67, was elevated in SSL-irradiated skin of *caspase-7* KO mice compared with those observed in SSL-exposed wild-type SKH1 mouse skin. Moreover, SSL-induced apoptosis was abolished in skin from *caspase-7* KO mice. Two-dimensional gel electrophoresis, followed by matrix-assisted laser desorption/ionization-time-of-flight analysis of skin tissue lysates from SSL-irradiated SKH1 wild-type and *caspase-7* KO mice revealed an aberrant induction of keratin-17 in *caspase-7* KO mice. Immunohistochemical analysis of skin tumors also showed an increase of keratin-17 expression in *caspase-7* KO mice compared with SKH1 wild-type mice. The expression of keratin-17 was also elevated in SSL-irradiated *caspase-7* KO keratinocytes as well as in human basal cell carcinomas. The *in vitro* caspase activity assay showed keratin-17 as a substrate of caspase-7, but not caspase-3. Overall, our study demonstrates that genetic loss of *caspase-7* promotes SSL-induced skin carcinogenesis by blocking caspase-7-mediated cleavage of keratin-17.

Received: February 24, 2015; **Revised:** July 10, 2015; **Accepted:** July 27, 2015

Abbreviations

2-DE	2-Dimensional gel electrophoresis
H&E	hematoxylin and eosin
IHC	immunohistochemistry
KO	knockout
MALDI	matrix-assisted laser desorption/ionization
MS	mass spectrometry
PBS	phosphate-buffered saline
PMSF	phenylmethylsulfonyl fluoride
SDS–PAGE	sodium dodecyl sulfate–polyacrylamide gel electrophoresis
SSL	solar-simulated light
TBS	Tris-buffered saline
TOF	time-of-flight
TUNEL	terminal dUTP nick-end labeling
UV	ultraviolet

Introduction

Solar ultraviolet (UV) irradiation, an environmental carcinogen, is a risk factor for non-melanoma skin cancers, including basal cell and squamous cell carcinomas (1–3). Solar UV irradiation (100–400 nm) can be divided into UVA (315–400 nm), UVB (280–315 nm) and UVC (100–280 nm) based on wavelength (4). Because UVC irradiation is absorbed by the atmospheric ozone layer, the solar UV irradiation that induces skin inflammation and carcinogenesis comprises a combination of UVA and UVB. Solar UV irradiation-induced oxidative DNA damage and genomic instability contribute to skin carcinogenesis but exposure to UV irradiation induces epidermal apoptosis. The induction of apoptosis tends to eliminate epidermal cells that harbor UV-induced genetic lesions and, hence, apoptosis is considered to be a protective mechanism against UV-induced skin carcinogenesis. Apoptosis, also known as programmed cell death, is executed by the activation of a series of proteolytic enzymes, including the cysteine–aspartic acid proteases (i.e. caspases). Cells harbor caspases in an inactive form (pro-caspases), which are activated through cleavage induced by appropriate death stimuli. The induction of apoptotic cell death involves two distinct mechanisms, death-receptor-mediated (i.e. extrinsic) and mitochondria-mediated (i.e. intrinsic) cell death. For the intrinsic-mediated pathway of apoptosis, a mitochondrial oxidative burst results in mitochondrial membrane depolarization and release of cytochrome c, which induces cleavage of pro-caspase-9, and initiates a cascade of cleavage of other pro-caspases, such as pro-caspase-3 and pro-caspase-7 (5). The activation of caspase-7, which is a common denominator of both the extrinsic and intrinsic pathways, leads to the induction of apoptosis. Previous studies have demonstrated that caspase-7 is deficient in several cancer types (6). In the present study, we investigated the impact and underlying mechanism of genetic ablation of *caspase-7* on solar-simulated light (SSL)-induced skin carcinogenesis compared with SKH1 wild-type mice. We report that depletion of *caspase-7* promotes UV-induced skin tumorigenesis at least partly by increasing the expression of keratin-17, an intermediate filament protein that stimulates proliferation of epidermal cells and promotes skin carcinogenesis.

Materials and methods

Reagents

Antibodies to detect pro and cleaved caspase-3, caspase-7 or caspase-9 were purchased from Cell Signaling Technology (Beverly, MA). The antibody against total β-actin or Ki-67 was purchased from Santa Cruz Biotechnology (Santa Cruz, CA) or Thermo Scientific (Fremont, CA), respectively. Antibodies to detect cystatin and keratin-17 were purchased from Epitomics (Burlingame, CA).

Generation of SKH1 caspase-7 knockout mice

Caspase-7 knockout (KO) mice (*Casp7tm1Fly:* Casp7$^{-/-}$), which are on the C57BL/6J genetic background, were purchased from Jackson Laboratories (Bar Harbor, ME) and maintained at The Hormel Institute University of Minnesota Animal Facility following the guidelines approved by the Animal Care and Use Committee (IACUC), University of Minnesota. The *Casp7*$^{-/-}$ mice were mated with SKH1 hairless mice on a Balb/c genetic background. The progenies, SKH1 caspase-7 heterozygotes (*Casp7*$^{+/-}$; filtered to 50% genetic background of SKH1 Balb/c hairless), were obtained by genomic PCR analysis using PCR primers, *oIMR5943*, *oIMR5944*, *oIMR5945* and *oIMR5946* according to recommended protocols. The *Casp7*$^{+/-}$ SKH1 caspase-7 heterozygote (*Casp7*$^{+/-}$) mice were continuously mated with SKH1 hairless mice until *Casp7*$^{+/-}$ genetic background was filtered to >95% of the SKH1 Balb/c hairless mice. Male and female *Casp7*$^{+/-}$ SKH1 mice were mated until homozygote mice (*Casp7*$^{-/-}$ SKH1) were obtained with 25% of Mendel's ratio. The *Casp7*$^{-/-}$ SKH1 mice were propagated and used for a SSL-induced skin tumorigenesis study. The genetic background of mice in each generation was determined by genomic PCR using the same primers described above.

Primary cultures of skin keratinocytes

Skin keratinocytes were isolated from 6- to 8-week-old mice and cultured as described previously (7). Briefly, mice were euthanized and dorsal skin sections were removed and treated with trypsin to detach the keratinocytes. Cells were harvested and seeded in collagen-coated dishes. After 72 h, culture medium was changed and keratinocytes were irradiated with different doses of SSL to determine dose-dependency or were irradiated with one dose of SSL and harvested at various times to determine a time course.

Western blot analysis

Cells were disrupted on ice for 30 min in cell lysis buffer [20 mM Tris, pH 7.5, 150 mM NaCl, 1 mM ethylenediaminetetraacetic acid, 1 mM ethylene glycol tetraacetic acid, 1% Triton X-100, 2.5 mM sodium pyrophosphate, 1 mM β-glycerophosphate, 1 mM sodium vanadate and 1 mM PMSF (phenylmethylsulfonyl fluoride)] and skin tissue samples were homogenized in lysis buffer [50 mM Tris–HCl pH 7.5, 150 mM NaCl, 2 mM ethylenediaminetetraacetic acid, 1% NP-40, 0.1% sodium dodecyl sulfate (SDS) and 1 mM PMSF]. After centrifugation at 13000 r.p.m. for 30 min, the supernatant fraction was harvested as the total cellular protein extract. The protein concentration was determined using the Bio-Rad protein assay reagent (Richmond, CA). The total cellular protein extracts were separated by SDS–polyacrylamide gel electrophoresis (PAGE) and transferred to polyvinylidene fluoride membranes in 20 mM Tris–HCl (pH 8.0), containing 150 mM glycine and 20% (vol/vol) methanol. Membranes were blocked with 5% non-fat dry milk in 1× Tris-buffered saline (TBS) containing 0.05% Tween 20 (TBS-T) and then incubated with antibodies. Blots were washed 3 times in 1× TBS-T buffer, followed by incubation with the appropriate horseradish peroxidase-linked IgG. Specific proteins were visualized using an enhanced chemiluminescence detection reagent.

SSL system

The SSL source comprised UVA-340 lamps purchased from Q-Lab Corporation (Cleveland, OH). The UVA-340 lamps provide the best possible simulation of sunlight in the critical short wavelength region from 365 nm down to the solar cutoff of 295 nm with a peak emission of 340 nm (8). The percentage of UVA and UVB of UVA-340 lamps was measured by a UV meter and was 94.5 and 5.5%, respectively.

Acute exposure of mice to SSL

Adult SKH1 wild-type and caspase-7 KO mice (6–8 weeks old, five per group for a total of three groups) were irradiated with 115 kJ/m^2 SSL. Dorsal trunk skin samples were harvested at 0 and 24 h after irradiation.

SSL-induced mouse skin carcinogenesis study

Skin carcinogenesis in mice was induced using UVA-340 lamps (Q-Lab Corporation). SKH1 wild-type and caspase-7 KO hairless mice were maintained at The Hormel Institute, University of Minnesota (Austin, MN).

Mice were maintained under conditions based on the guidelines established by the Institutional Animal Care and Use Committee, University of Minnesota. The mice were divided into 4 groups of 20 animals each (6–8 weeks old, with an average body weight of 25 g). For untreated control groups, SKH1 wild-type and caspase-7 KO mice were not irradiated with SSL. For the experimental SSL-treated groups, SKH1 wild-type and caspase-7 KO mice were initially treated with an SSL dose of 30 kJ UVA/m^2–1.8 kJ UVB/m^2 twice a week. The dose was increased by 10% each week until week 6. At week 6, the dose reached 48 kJ UVA/m^2–2.9 kJ UVB/m^2, and this dose was maintained from weeks 6 to 10. At 10 weeks, SSL exposure was discontinued, and tumor growth was monitored for an additional 15 weeks. A tumor was defined as an outgrowth of >1 mm in diameter. Tumor numbers and volume were recorded every week until the end of the experiment. Tumor volume was calculated according to the following formula: tumor volume (mm^3) = length × width × height × 0.52. Skin and tumors were harvested and one-half of the samples were immediately fixed in 10% neutral-buffered formalin and processed for hematoxylin and eosin (H&E) staining and immunohistochemistry (IHC). The other half was frozen for western blot analysis.

Terminal dUTP nick-end labeling, H&E staining and IHC

Skin tissues from mice were embedded in paraffin blocks and subjected to terminal dUTP nick-end labeling (TUNEL), H&E staining and IHC. Tumor tissues were deparaffinized and hydrated and then permeabilized with 0.5% Triton X-100/1 × phosphate-buffered saline (PBS) for 10 min. Apoptotic cells in skin tissues were identified by TUNEL staining using a DeadEnd™ Fluorometric TUNEL System (Promega, Madison, WI) or FragEL™ DNA Fragmentation Detection Kit (Colorimetric) (Millipore Corporation, Billerica, MA) according to the manufacturer's instructions. Tissues were then hybridized with Ki-67 (1:50) or keratin-17 (1:200) as the primary antibody and a biotinylated goat anti-rabbit or mouse IgG antibody was used as the secondary antibody. The ABC kit (Vector Laboratories, Inc., Burlingame, CA) was used to detect the protein targets according to the manufacturer's instructions. After developing with 3, 3′-diaminobenzidine, the sections were counterstained with hematoxylin. All sections were observed by microscope (×200 magnification) and analyzed with the Image-Pro Plus software (v. 6.1) program (Media Cybernetics, Rockville, MD).

Immunohistochemical staining of skin tissue microarrays

A human skin tissue array (SK801) was purchased from US Biomax (Rockville, MD) and tissue analysis was conducted according to the manufacturer's suggested protocols. The tissue array included matched normal tissues (H1–H7), which were biopsied from the adjacent tissue of each cancer tissue (A1–A7) from seven individual patients. A Vectastain Elite ABC Kit (Vector Laboratories) was used for immunohistochemical staining according to the recommended protocol. Briefly, the slide was baked at 60°C for 2 h, deparaffinized and rehydrated. To expose antigens, the slide was unmasked by submersion into boiling sodium citrate buffer (10 mM, pH 6.0) for 10 min and then treated with 3% H_2O_2 for 10 min. The slide was blocked with 5% goat serum albumin in 1× PBS in a humidified chamber for 1 h at room temperature and then with a keratin-17 antibody (1:100 dilution in 3% goat serum with PBS) at 4°C in a humidified chamber overnight. The slide was washed and hybridized with a secondary antibody from Vector Laboratories (anti-rabbit 1:500) for 1 h at room temperature. Slides were stained using the Vectastain Elite ABC kit. All sections were observed by microscope (×200 magnification). The intensity of IHC staining was quantified by calculating the integrated optical density using the Image Pro-Plus 7.0 software program (Media Cybernetics, Bethesda, MD).

2-Dimensional gel electrophoresis

2-Dimensional gel electrophoresis (2-DE) was conducted essentially as described (9,10). Aliquots in sample buffer (7 M urea, 2 M thiourea, 4.5% [(3-cholamidopropyl)-dimethyl-ammonio]1-propanesulfonate, 100 mM dithioerythritol and 40 mM Tris, pH 8.8) were applied to immobilized pH 3–10 non-linear gradient strips (Amersham Biosciences, Uppsala, Sweden). Isoelectric focusing was performed at 80000 Vh. The second dimension was analyzed on 9–16% linear gradient polyacrylamide gels (18 cm × 20 cm × 6 1.5 mm) at constant 40 mA per gel for ~5 h. After protein fixation in 40% methanol and 5% phosphoric acid for 1 h, the gels were stained with CBB G-250 for 12 h. The gels were destained with H_2O, scanned in a Bio-Rad GS710 densitometer and converted into electronic files, which were then analyzed with Image Master Platinum 5.0 image analysis software (Amersham Biosciences).

Matrix-assisted laser desorption/ionization-time-of-flight analysis

For MALDI-TOF-MS (matrix-assisted laser desorption/ionization-time-of-flight-mass spectrometry) analysis, the peptides were concentrated using a POROS R2, Oligo R3 column (Applied Biosystems, Foster City, CA). After washing the column with 70% acetonitrile, 100% acetonitrile and then 50 mM ammonium bicarbonate, samples were applied to the R2, R3 column and eluted with cyano-4-hydroxycinnamic acid (Sigma, St Louis, MO) dissolved in 70% acetonitrile and 2% formic acid onto the MALDI plate (Opti-TOF™ 384-well Insert; Applied Biosystems) (11). MALDI-TOF-MS was performed on a 4800 MALDI-TOF/TOF™ Analyzer (Applied Biosystems) equipped with a 355 nm Nd:YAG laser. The pressure in the TOF analyzer was ~7.6e-07 Torr. The mass spectra were obtained in the reflectron mode with an accelerating voltage of 20 kV and summed from either 500 laser pulses and calibrated using the 4700 calibration mixture (Applied Biosystems).

Mascot database search

Database search criteria were: taxonomy, *Mus*., fixed modification; carboxyamidomethyl (+57) at cysteine residues; variable modification; oxidized (+16) at methionine residues, maximum allowed missed cleavage, 1, MS tolerance, 100 p.p.m. Only peptides resulting from trypsin digests were considered.

In vitro cleavage of keratins with recombinant caspases

Cleavage reactions with recombinant caspases-3 or -7 (PromoCell, Heidelberg, Germany) were performed with 20 µl caspase buffer (50 mM *N*-2-hydroxyethylpiperazine-*N*′-2-ethanesulfonic acid, pH 7.4, 0.1% [(3-cholamidopropyl)-dimethyl-ammonio]1-propanesulfonate, 5 mM dithiothreitol, 1 mM PMSF, 50 mM leupeptin, 200 µg/ml aprotinin) at 30°C for 3 h using keratin-5 or -17 as a substrate that was transcribed from the pET-24-mKeratin-5 or pET3d-mKeratin-17 (a kind gift from Dr Pierre A.Coulombe, Johns Hopkins University, Baltimore, MD) and translated using the TNT Quick Coupled Transcription/Translation System (Promega) in the presence of [^{35}S]-methionine. The translation mixture (2 µl) was used for the cleavage reaction with the recombinant caspases described above. Samples were separated by 12% SDS–PAGE. [^{35}S]-labeled proteins were detected by autoradiography.

Statistical analyses

All quantitative results are expressed as mean values ± SD. Statistically significant differences were obtained using the Student's *t*-test or one-way analysis of variance. A value of $P < 0.05$ was considered to be statistically significant.

Results

SSL induces epidermal cell death in normal SKH1 wild-type mice, but not in caspase-7 KO mice

The induction of apoptosis is largely mediated through the activation of a series of caspases including caspase-9, -3 and -7. In an effort to examine the role of caspase-7 in SSL-induced skin carcinogenesis, we first investigated the effect of genetic ablation of *caspase-7* on SSL-induced apoptosis in mouse skin. We irradiated normal SKH1 wild-type and *caspase-7*-KO mouse skin with SSL (115 kJ/m^2) and examined epidermal skin thickness and apoptosis at 24 h post-irradiation. Results indicated that epidermal thickness in *caspase-7* KO

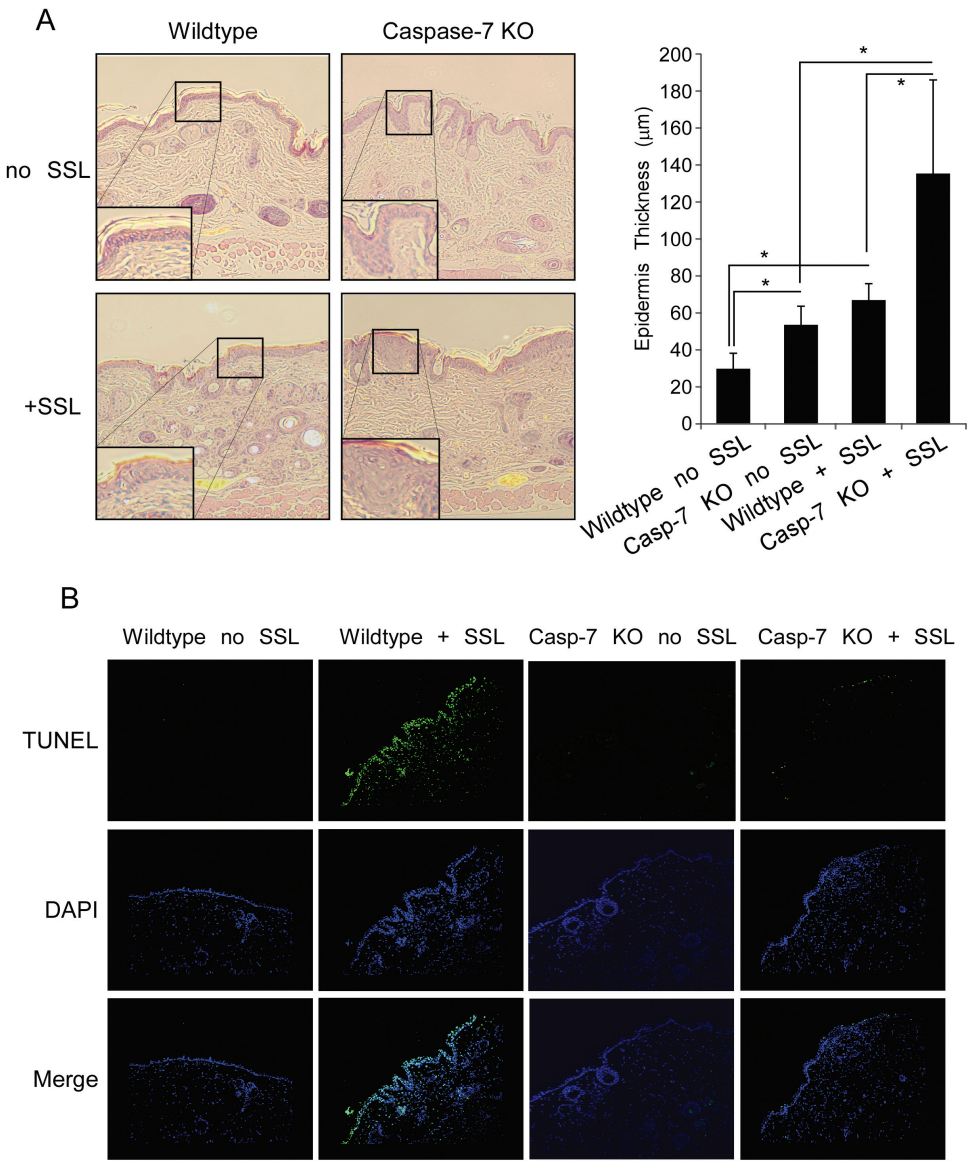

Figure 1. Skin thickness and induction of apoptosis in acute SSL-treated SKH1 wild-type and caspase-7 KO mice. (**A**) Epidermal skin thickness in mice treated or not treated with SSL (115 kJ/m^2). After H&E staining of skin samples, epidermal skin thickness was analyzed in five separate areas using EZ-C1 FreeViewer Gold software (v. 3.2; Nikon, Melville, NY) and an average of three samples was calculated per group. Data are shown as mean values ± SD. The asterisk (*) indicates a significant ($P < 0.05$) increase in epidermal skin thickness. (**B**) The induction of apoptosis in untreated mouse skin or in skin from mice treated with SSL was analyzed by TUNEL assay. Apoptotic cells in skin tissue samples were detected according to the instructions provided by the manufacturer as described in Materials and methods section. Similar results were obtained from three samples per group.

mice was significantly greater than that of SKH1 wild-type mice even without exposure to SSL (Figure 1A). Whereas SSL caused significantly increased epidermal thickness in SKH1 wild-type mouse skin compared to non-irradiated skin, a several-fold increase in epidermal skin thickness was observed in SSL-treated *caspase-7* KO mouse skin. In agreement with the increased epidermal skin thickness, TUNEL assay results revealed that SSL-induced apoptosis was markedly attenuated in *caspase-7* KO mouse skin compared to that observed in SKH1 wild-type mouse skin with exposure to SSL (Figure 1B).

Genetic ablation of caspase-7 enhances SSL-induced skin carcinogenesis

We then determined whether the deletion of *caspase-7* and the resultant SSL-induced increase in epidermal skin thickness and marked inhibition of apoptosis might affect SSL-induced skin carcinogenesis in *caspase-7* KO mice. SKH1 wild-type and *caspase-7* KO mice were subjected to irradiation with SSL or unexposed for 10 weeks. SSL treated was then discontinued and tumor growth monitored for an additional 15 weeks. Skin tumor volume and number were monitored until the termination of the experiment at week 25. Analyses of tumor data revealed that the volume and the average number of skin tumors were significantly increased in SSL-treated SKH1 wild-type mice compared to untreated animals, which validated the experimental protocol for SSL-induced skin carcinogenesis. Compared to normal SKH1 wild-type mice, the volume (Figure 2A) and average number (Figure 2B) of tumors in SSL-exposed *caspase-7* KO mice were significantly higher, suggesting that the deficiency of *caspase-7* sensitizes mouse skin to SSL-induced carcinogenesis. H&E staining of skin

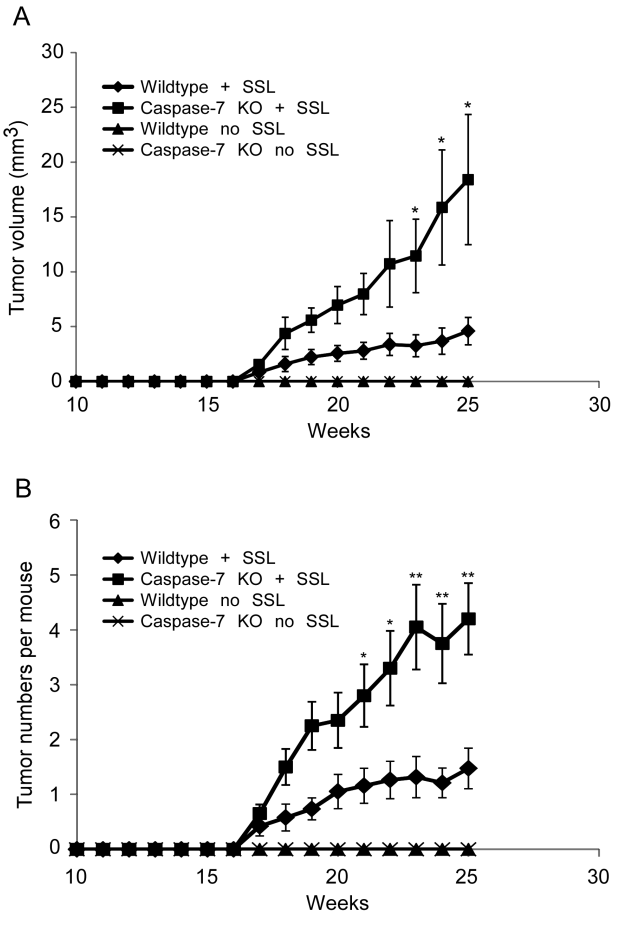

Figure 2. Tumor volume and numbers in SKH1 wild-type or caspase-7 KO mice untreated or treated with SSL. (**A**) Average tumor volume and (**B**) tumor number per mouse. Mice were treated with SSL for 10 weeks and then monitored for a total of 25 weeks. Tumor volume and numbers were measured each week until 25 weeks. Tumors first appeared at 17 weeks. Data are shown as mean values ± SE. The asterisk indicates a significant increase in tumor volume and number (*$P < 0.05$; **$P < 0.01$) in caspase-7 KO mice compared to untreated SKH1 wild-type mice or mice treated with SSL. No tumors developed in untreated mice.

tissues showed that chronic exposure to SSL increased the epidermal skin thickness more dramatically in *caspase-7* KO mice compared to SKH1 wild-type mice (Figure 3A). In addition, immunohistochemical analysis revealed an increased expression of Ki-67, a proliferation marker, in SSL-exposed *caspase-7* KO mouse skin compared to SKH1 wild-type mouse skin (Figure 3B). Immunoblot analysis of epidermal tissue lysates showed that exposure to long-term SSL induced cleavage of caspase-3 or -7 in normal SKH1 wild-type mice, but the SSL-induced caspase-3 cleavage was more intense in *caspase-7* KO mouse skin (Figure 3C). Compared to SKH1 wild-type mice, irradiation with SSL caused a significant increase in the expression of survivin, another cell proliferation marker, in *caspase-7* KO mice (Figure 3C, lower panel). Although the expression of oncogenic p23 remained unchanged in unexposed SKH1 wild-type and *caspase-7* KO mice, an increase in the level of p23 was observed in SSL-exposed *caspase-7* KO mouse skin compared to that of untreated *caspase-7* KO mice (Figure 3C, middle panel). Although exposure to SSL induced apoptosis in SKH1 wild-type mouse skin, as revealed by the presence of TUNEL-positive cells, the *caspase-7* KO mouse skin showed no signs of apoptosis upon irradiation with SSL (Figure 3D).

Effect of SSL irradiation on the cleavage of caspases in SKH1 wild-type or caspase-7 KO keratinocytes

To elucidate the underlying molecular mechanisms of enhanced skin tumorigenesis in SSL-exposed *caspase-7* KO mice, we isolated keratinocytes from both SKH1 wild-type and *caspase-7* KO mice and optimized the intensity and exposure time of SSL that can cause cleavage of execution caspases. Results revealed that exposure to SSL induced cleavage of caspases in a dose- and time-dependent manner (Figure 4A and B). Irradiation with SSL caused maximal induction of caspase-7 and -3 cleavage at a dose of 48 kJ/m^2 in keratinocytes isolated from normal SKH1 wild-type mice 24 h post-irradiation (Figure 4A). A similar pattern of SSL-induced caspase-3 cleavage was noted in keratinocytes obtained from *caspase-7* KO mice (Figure 4A). A kinetic study revealed that irradiation with SSL (48 kJ/m^2) induced the cleavage of caspase-9, -3 or -7 in wild-type keratinocytes and the cleavage of caspase-9 and -3 in *caspase-7* KO keratinocytes at 24 h after exposure (Figure 4B).

Involvement of keratin-17 in SSL-induced tumor promotion in caspase-7 KO mice

To identify a molecular target of caspase-7, we irradiated wild-type and *caspase-7* KO mice with SSL and prepared skin tissue lysates for 2-DE. By comparing and analyzing 2-DE gel images, we marked spots that were changed by more than 2-fold and identified 71 spots by MALDI-TOF analysis (Figure 5A). A list of 23 proteins (Supplementary Table S1, available at *Carcinogenesis* Online) that exhibited a marked alteration in their expression pattern between SKH1 wild-type and *caspase-7* KO mice after irradiation with SSL were noteworthy for further analysis. One spot identified as cystatin (Figure 5B, arrow), a protein overexpressed in various cancers (12), was induced in both SSL-irradiated SKH1 wild-type and *caspase-7* KO mouse skin. The SSL-induced cystatin expression was more pronounced in *caspase-7* KO mice than in SKH1 wild-type mice. Likewise, the expression of keratin-17 was 4.7-fold higher in SSL-irradiated *caspase-7* KO mice (Figure 5C, arrow). The increased expression of keratin-17 was confirmed by western blotting with each tissue sample (Figure 5D). Bands were quantified and are shown as mean values ± SD (lower panels). To assess the status of keratin-17 expression in skin cancer, we analyzed a tissue microarray of skin cancer. Results showed that keratin-17 was overexpressed in basal cell carcinoma compared to normal tissues. In addition, the expression of keratin-17 was also significantly increased in squamous cell carcinoma and malignant melanoma, but not to the same extent as basal cell carcinoma. (Figure 5E; Supplementary Figure S1, available at *Carcinogenesis* Online). Immunohistochemical analysis of skin sections revealed that the expression of keratin-17 was also increased in acute SSL-irradiated *caspase-7* KO mouse skin (Figure 5F).

Keratin-17 is a direct target of caspase-7

To determine whether keratin-17 is a direct target of caspase-7, we performed an *in vitro* enzyme activity assay. Recombinant caspase-3 and -7 were separately incubated with keratin-5 or keratin-17 as substrates (Figure 6; Supplementary Figure S2, available at *Carcinogenesis* Online). Results showed that incubation with caspase-7, but not with caspase-3, caused cleavage of keratin-17 (Figure 6). While caspase-7 induced cleavage of keratin-17, it did not cause cleavage of keratin-5 (Supplementary Figure S2, available at *Carcinogenesis* Online). These findings indicate that keratin-17 is a direct target of caspase-7.

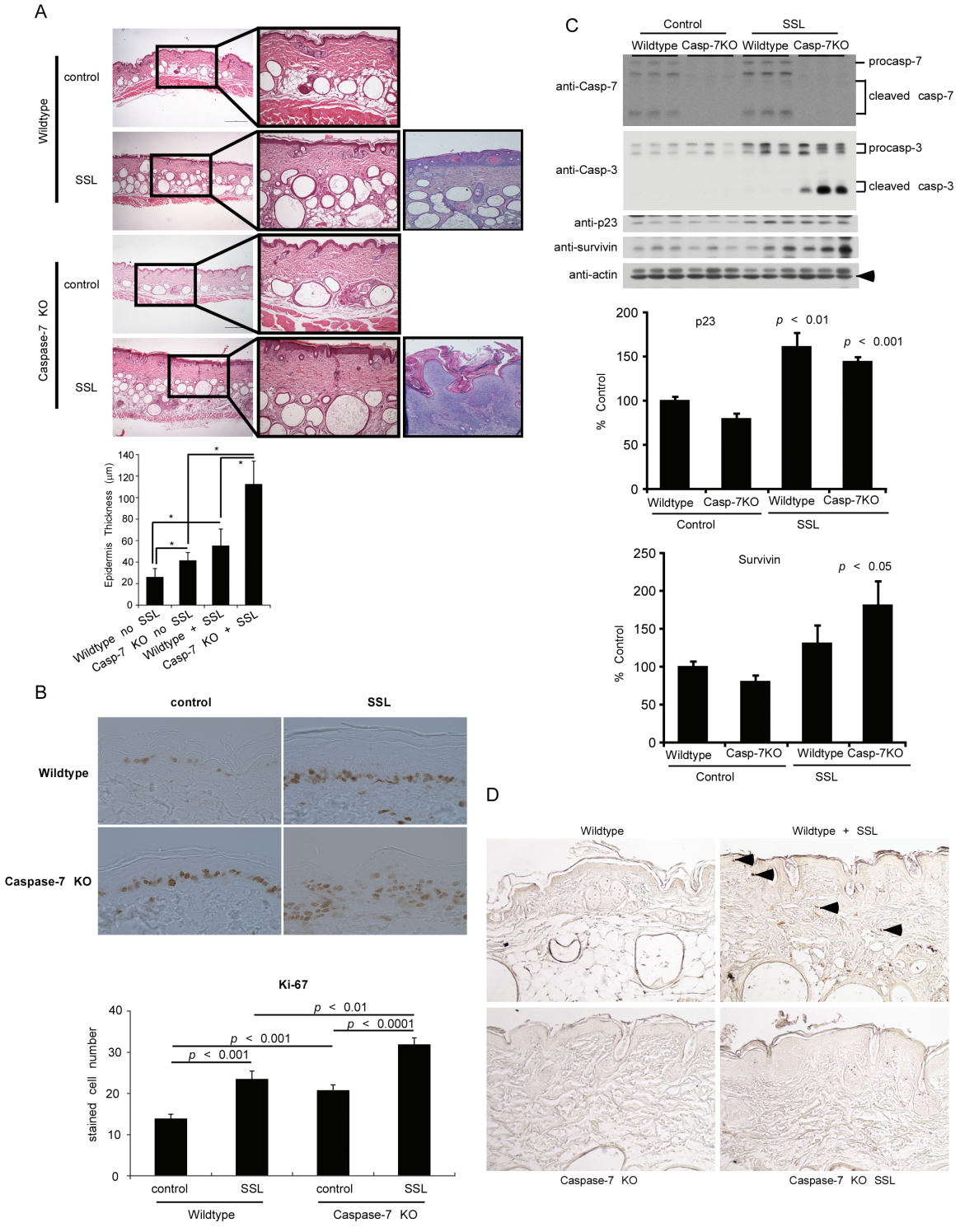

Figure 3. Epidermal skin thickness, expression of Ki-67 and induction of apoptosis in long-term SSL-treated SKH1 wild-type and caspase-7 KO mice. (**A**) Epidermal skin thickness after treatment with SSL. After H&E staining of skin samples, epidermal thickness was analyzed in five separate areas using EZ-C1 FreeViewer Gold software (v. 3.20; Nikon) and an average of three samples was calculated per group. Data are shown as mean values ± SD. The asterisk (*) indicates a significant ($P < 0.05$) increase in skin thickness. (**B**) Ki-67 expression was detected by IHC and significant changes are noted in the lower panel. (**C**) The expression of caspase-3, -7, p23 and survivin was detected by western blotting (upper panels). Significant changes in p23 and survivin are indicated (lower panels). (**D**) The induction of apoptosis after treatment with SSL detected by TUNEL assay. Apoptotic cells in skin tissue samples were detected (arrows) following the manufacturer's instructions (Millipore Corporation, Billerica, MA). Similar results were obtained from three samples per group.

Discussion

Apoptosis induced by UV irradiation is one of the physiological phenomena observed in skin carcinogenesis (13–15). Caspase-7, a key player in apoptosis, is reportedly linked to many types of human cancers. Our results indicated that tumor volume and number were more pronounced in SSL-treated caspase-7

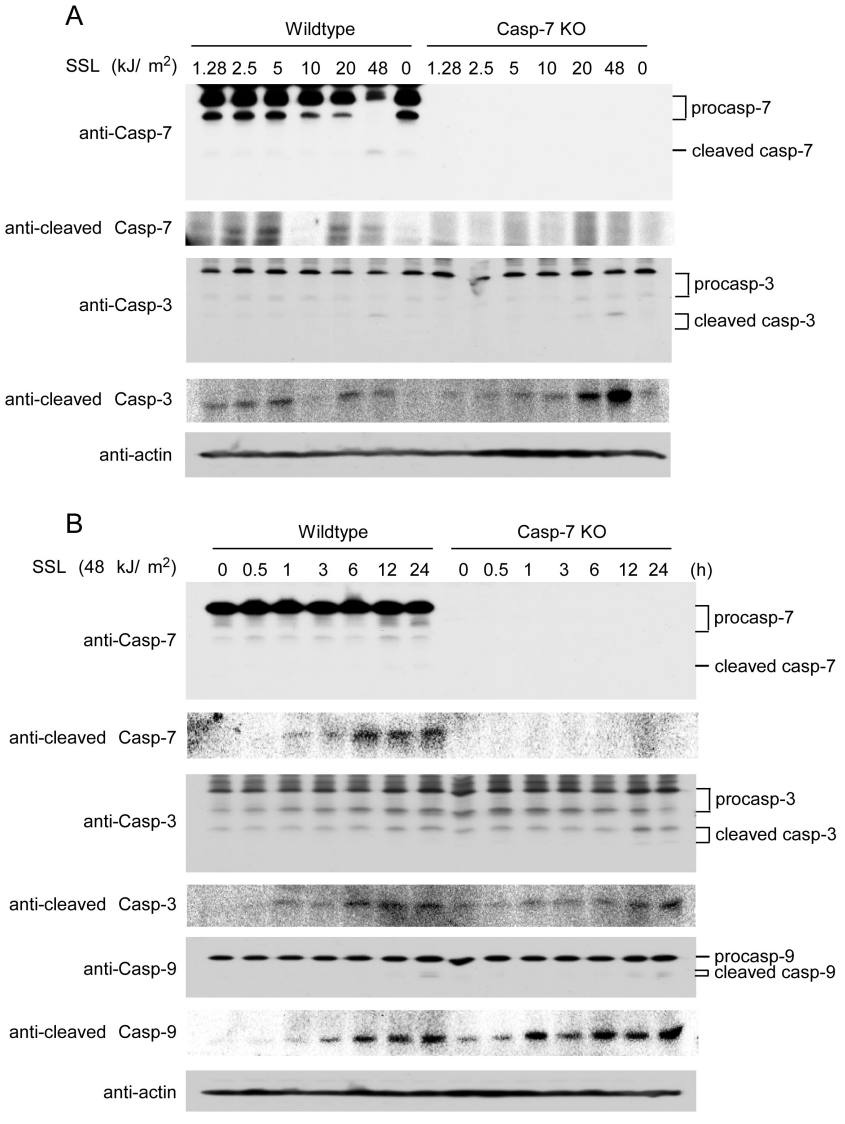

Figure 4. The expression of caspases in SSL-treated keratinocytes. (**A**) Cleaved caspase-3 and -7 expression in SSL-treated SKH1 wild-type or caspase-7 KO keratinocytes treated with increasing doses of SSL. (**B**) Cleaved caspase-3, -7 and -9 expression in SSL-treated SKH1 or caspase-7 KO keratinocytes over a time course. For dose-dependency, primary keratinocytes were treated with doses of SSL at 0, 1.28, 2.5, 5, 10, 20 or 48 kJ/m^2 and after 24 h, cells were harvested and examined by western blotting. For time course assessment, primary keratinocytes were treated with SSL at 48 kJ/m^2 and harvested at 0, 0.5, 1, 3, 6, 12 or 24 h and proteins were detected. Similar results were obtained from two independent experiments.

KO mice compared with SSL-treated SKH1 wild-type mice (Figure 2A and B). The expression of cleaved caspase-3 was higher in SSL-treated caspase-7 KO keratinocytes and mice compared to wild-type (Fig. 3C, 4A and B). However, this might not be a complementary enhancement but rather an accumulation of caspase-3 caused by a blockade of downstream signaling because caspase-7 is a downstream signaling protein of caspase-3 (16). Thus, a dysfunctional caspase-7 might lead to more inflammation and cancer because of resistance to apoptosis. This suggests that caspase-7 is a critically important protein in SSL-induced apoptosis. Although caspase-7 KO mice are normal in appearance, organ morphology and lymphoid development (17), we found that the epidermal skin thickness of caspase-7 KO mice was thicker than that of SKH1 wild-type mice (Figures 1A and 3A). Our 2-DE gel and MALDI-TOF results indicated that keratin-17 was markedly increased in skin from SSL-treated SKH1 wild-type mice compared to SSL-treated caspase-7 KO mice (see Supplementary Table S1, available at *Carcinogenesis* Online). We also classified proteins identified by mass spec by function, and keratin-17 is notably involved in molecular functions and biological process and is an important cellular component [see Supplementary Table S2, available at *Carcinogenesis* Online; (18,19)]. Keratin-17 is a type I filament protein that is involved in epithelial proliferation, tumor growth and angiogenesis (20–22). Notably, results of an *in vitro* caspase enzyme assay indicated that keratin-17 was cleaved by caspase-7 but not by caspase-3. This suggests that keratin-17 is a specific substrate of caspase-7. In the past, caspase-3 and caspase-7 have been widely believed to possess a similar substrate spectrum, including recognition of tetra-peptide (X-X-X-Asp) motifs, cutting the C-terminal of Asp and redundant functionality (23). On the other hand, numerous studies have suggested that caspase-3 and caspase-7 have different functions, given that caspase-3 KO mice are embryonic lethal, whereas caspase-7 KO mice are viable (24–26). These findings led us to determine whether caspase-7 is a specific protease for keratin-17. In the present study, we found

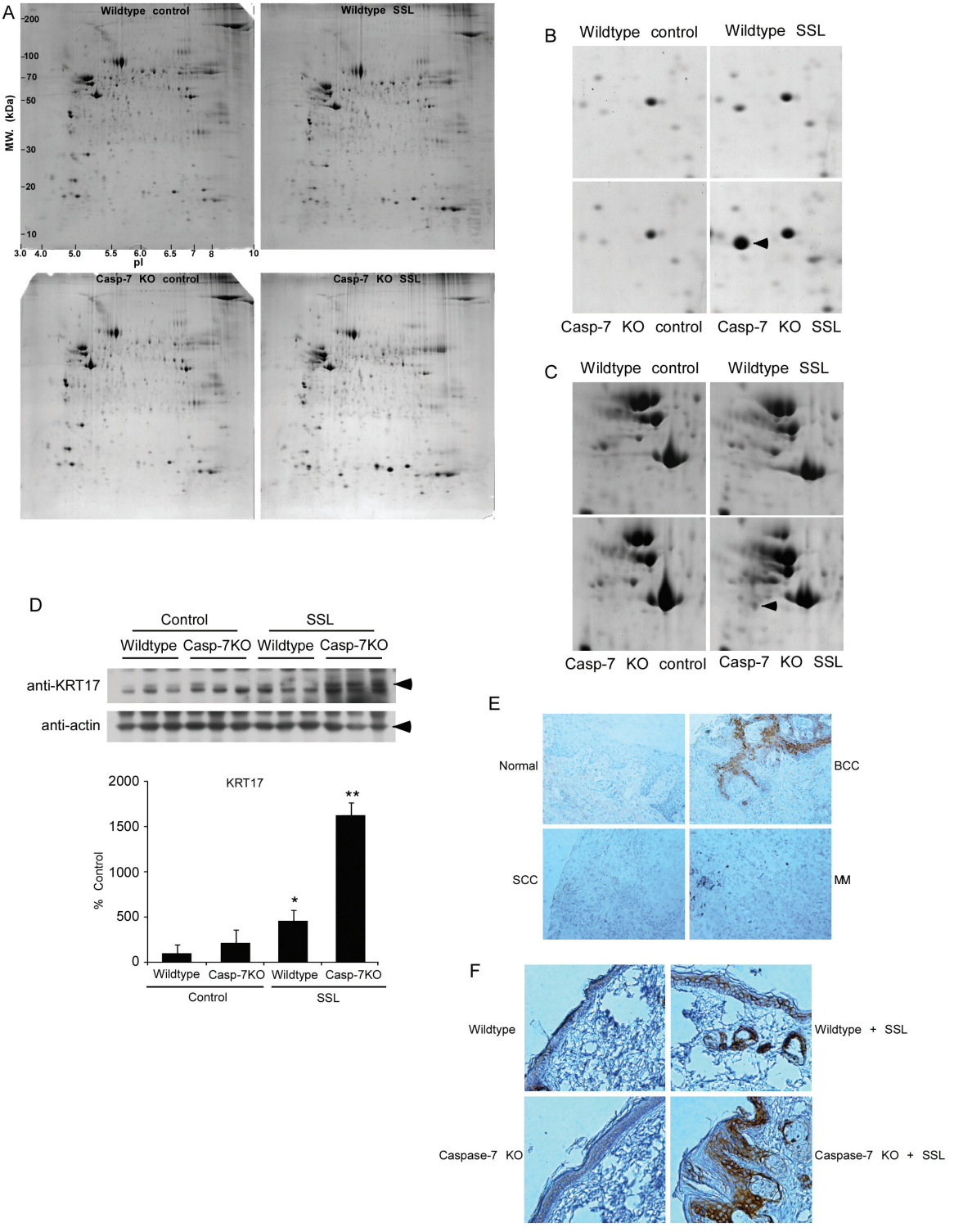

Figure 5. An investigation of target proteins. (**A**) 2-DE analysis of SKH1 wild-type and caspase-7 KO mouse skin. (**B**) A spot (arrow) is identified as cystatin. (**C**) A spot (arrow) is identified as keratin-17. (**D**) Western blot analysis of the expression of keratin-17 and β-actin in skin tissue samples. In the lower panel, the bands were quantified using the image J software program (NIH). Data are shown as mean values ± SD. The asterisk indicates a significant increase of expression (*$P < 0.05$; **$P < 0.01$) in caspase-7 KO mice compared to untreated control. The expression of keratin-17 in a skin tissue microarray (**E**) or acute SSL-treated skin samples (**F**).

that keratin-17 is a specific substrate of caspase-7, but not caspase-3. Furthermore, keratin-17 was up-regulated in caspase-7 KO mice compared to wild-type mice. Thus, keratin-17, which is cleaved by caspase-7, but not caspase-3, could be used as a biomarker for skin cancer patients with caspase-7 malfunction. Overall, our results strongly indicate that caspase-7 acts as an executioner protein in the regulation of SSL-induced skin carcinogenesis acting by down-regulating keratin-17.

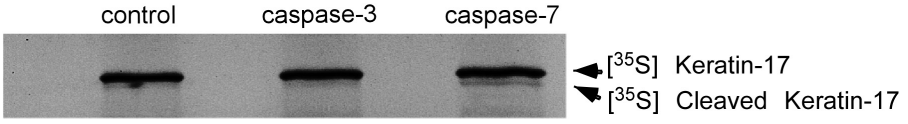

Figure 6. Enzymatic activity of caspases against keratin-17. Radioactive-labeled keratin-17 was translated using the TNT Quick Coupled Transcription/Translation System in the presence of [^{35}S]-methionine. Cleavage reactions were performed with or without recombinant caspase-3 or -7 as described in Materials and methods. Samples were separated by 12% SDS–PAGE. [^{35}S]-labeled proteins were detected by autoradiography. The upper band indicates intact [^{35}S] keratin-17 and the lower band designates cleaved [^{35}S] keratin-17.

Supplementary material

Supplementary Tables S1 and S2 and Figures S1 and S2 can be found at http://carcin.oxfordjournals.org/

Funding

The Hormel Foundation and National Institutes of Health grants (CA027502, ES016548, CA166001 and CA172457 to Z.D.); Ministry of Science, ICT and Future Planning (2012M3A9B6055466 to Y.Y.C.); Basic Science Research Program through the National Research Foundation of Korea (NRF) funded by the Ministry of Education (2013R1A1A2057487 to M.H.L.).

Acknowledgements

We thank Wei-ya Ma, Jin Young Suh, Jong Eun Kim, Dong Hoon Yu, Naomi Oi, Andria Carper and Alyssa Langerud for supporting experiments (The Hormel Institute, University of Minnesota). We wish to acknowledge technical support from the Yonsei Proteome Research Center (www.proteomix.org).
Conflict of Interest Statement: None declared.

References

1. Beissert, S. et al. (2008) Molecular and cellular mechanisms of photocarcinogenesis. Photochem. Photobiol., 84, 29–34.
2. Berking, C. (2007) Photocarcinogenesis. Molecular mechanisms and preventive strategies. Hautarzt., 58, 398–405.
3. Diffey, B.L. (1991) Solar ultraviolet radiation effects on biological systems. Phys. Med. Biol., 36, 299–328.
4. Diffey, B.L. (2002) Sources and measurement of ultraviolet radiation. Methods, 28, 4–13.
5. Elmore, S. (2007) Apoptosis: a review of programmed cell death. Toxicol. Pathol., 35, 495–516.
6. Soung, Y.H. et al. (2003) Inactivating mutations of CASPASE-7 gene in human cancers. Oncogene, 22, 8048–8052.
7. Watt, F.M. (1994) Keratinocyte Method. Cambridge University Press, New York, NY.
8. Nakano, H. et al. (2001) UVA-340 as energy source, mimicking natural sunlight, activates the transcription factor AP-1 in cultured fibroblasts: evidence for involvement of protein kinase-C. Photochem. Photobiol., 74, 274–282.
9. Park, K.S. et al. (2002) Proteomic analysis and molecular characterization of tissue ferritin light chain in hepatocellular carcinoma. Hepatology, 35, 1459–1466.
10. Park, K.S. et al. (2002) Proteomic alterations of the variants of human aldehyde dehydrogenase isozymes correlate with hepatocellular carcinoma. Int. J. Cancer, 97, 261–265.
11. Choi, B.K. et al. (2003) Single-step perfusion chromatography with a throughput potential for enhanced peptide detection by matrix-assisted laser desorption/ ionization-mass spectrometry. Proteomics, 3, 1955–1961.
12. Keppler, D. (2006) Towards novel anti-cancer strategies based on cystatin function. Cancer Lett., 235, 159–176.
13. Kulms, D. et al. (2000) Molecular mechanisms of UV-induced apoptosis. Photodermatol. Photoimmunol. Photomed., 16, 195–201.
14. Rodust, P.M. et al. (2009) UV-induced squamous cell carcinoma–a role for antiapoptotic signalling pathways. Br. J. Dermatol., 161(suppl. 3), 107–115.
15. Lee, C.H. et al. (2013) Molecular mechanisms of UV-induced apoptosis and its effects on skin residential cells: the implication in UV-based phototherapy. Int. J. Mol. Sci., 14, 6414–6435.
16. Fernandes-Alnemri, T. et al. (1995) Mch3, a novel human apoptotic cysteine protease highly related to CPP32. Cancer Res., 55, 6045–6052.
17. Lakhani, S.A. et al. (2006) Caspases 3 and 7: key mediators of mitochondrial events of apoptosis. Science, 311, 847–851.
18. Huang da, W., et al. (2009) Systematic and integrative analysis of large gene lists using DAVID bioinformatics resources. Nat Protoc, 4, 44–57.
19. Huang da, W., et al. (2009) Bioinformatics enrichment tools: paths toward the comprehensive functional analysis of large gene lists. Nucleic Acids Res., 37, 1–13.
20. Kim, S. et al. (2006) A keratin cytoskeletal protein regulates protein synthesis and epithelial cell growth. Nature, 441, 362–365.
21. Xu, Y. et al. (2009) Keratin 17 identified by proteomic analysis may be involved in tumor angiogenesis. BMB Rep., 42, 344–349.
22. Depianto, D. et al. (2010) Keratin 17 promotes epithelial proliferation and tumor growth by polarizing the immune response in skin. Nat. Genet., 42, 910–914.
23. Stennicke, H.R. et al. (2000) Internally quenched fluorescent peptide substrates disclose the subsite preferences of human caspases 1, 3, 6, 7 and 8. Biochem. J., 350(Pt 2), 563–568.
24. Kuida, K. et al. (1996) Decreased apoptosis in the brain and premature lethality in CPP32-deficient mice. Nature, 384, 368–372.
25. Houde, C. et al. (2004) Caspase-7 expanded function and intrinsic expression level underlies strain-specific brain phenotype of caspase-3-null mice. J. Neurosci., 24, 9977–9984.
26. Walsh, J.G. et al. (2008) Executioner caspase-3 and caspase-7 are functionally distinct proteases. Proc. Natl. Acad. Sci. USA, 105, 12815–12819.